Clinical Chemistry 53:11
1891–1898 (2007)

Molecular Diagnostics and Genetics

Scanning the Cystic Fibrosis Transmembrane Conductance Regulator Gene Using High-Resolution DNA Melting Analysis

Jesse Montgomery,[1] Carl T. Wittwer,[1,2*] Jana O. Kent,[1] and Luming Zhou[1]

Background: **Complete gene analysis of the cystic fibrosis transmembrane conductance regulator gene (*CFTR*) by scanning and/or sequencing is seldom performed because of the cost, time, and labor involved. High-resolution DNA melting analysis is a rapid, closed-tube alternative for gene scanning and genotyping.**

Methods: **The 27 exons of *CFTR* were amplified in 37 PCR products under identical conditions. Common variants in 96 blood donors were identified in each exon by high-resolution melting on a LightScanner®. We then performed a subsequent blinded study on 30 samples enriched for disease-causing variants, including all 23 variants recommended by the American College of Medical Genetics and 8 additional, well-characterized variants.**

Results: **We identified 22 different sequence variants in 96 blood donors, including 4 novel variants and the disease-causing p.F508del. In the blinded study, all 40 disease-causing heterozygotes (29 unique) were detected, including 1 new probable disease-causing variant (c.3500-2A>T). The number of false-positive amplicons was decreased 96% by considering the 6 most common heterozygotes. The melting patterns of most heterozygotes were unique (37 of 40 pairs within the same amplicon), the exceptions being p.F508del vs p.I507del, p.G551D vs p.R553X, and p.W1282X vs c.4002A>G. The homozygotes p.G542X, c.2789 + 5G>A, and c.3849 + 10kbC>T were directly identified, but homozygous p.F508del was not. Specific genotyping of these exceptions, as well as genotyping of the 5T allele of intron 8, was achieved by unlabeled-probe and small-amplicon melting assays.**

Conclusions: **High-resolution DNA melting methods provide a rapid and accurate alternative for complete *CFTR* analysis. False positives can be decreased by considering the melting profiles of common variants.**

Since the identification of the cystic fibrosis transmembrane conductance regulator gene (*CFTR*)[3] in 1989 *(1)*, more than 1500 variants have been identified (http://www.genet.sickkids.on.ca/cftr). The frequency and distribution of disease-causing variants differ remarkably across ethnicities and geographical locations. For example, the allele frequency of p.F508del (ΔF508) in cystic fibrosis ranges from as high as 100% in the Faroe Islands of Denmark to as low as 24.5% in Turkey *(2)*. In the Netherlands only 9 mutations occur at frequencies >0.5%, whereas in Greece 22 mutations occur. Several common mutations are specific to ethnic groups, such as p.W1282X among Ashkenazi Jews and c.3120 + 1G>A among native Africans.

Genotyping panels are commonly used to screen for cystic fibrosis. The selection of variants is difficult, however, because of ethnic and geographic diversity. In 2001, the American College of Medical Genetics (ACMG)[4] recommended a screening panel for the US *(3)* that included 25 mutations with an estimated frequency of at least 0.1%. Although the screening panel was designed to be panethnic, the estimated detection rates were 97%, 80%, 69%, and 57% for Ashkenazi Jewish, white European, African American, and Hispanic American populations, respectively. With increasing ethnic admixture and limited

[1] Department of Pathology, University of Utah Health Sciences Center, Salt Lake City, UT.
[2] ARUP Institute for Clinical and Experimental Pathology, Salt Lake City, UT.
* Address correspondence to this author at: Department of Pathology, University of Utah Medical School, 50 N. Medical Dr., Salt Lake City, UT 84132. Fax 801-581-6001; e-mail carl.wittwer@path.utah.edu.
Received May 20, 2007; accepted August 20, 2007.
Previously published online at DOI: 10.1373/clinchem.2007.092361

[3] Human gene: *CFTR*, cystic fibrosis transmembrane conductance regulator (ATP-binding cassette sub-family C, member 7).
[4] Nonstandard abbreviations: ACMG, American College of Medical Genetics; ARUP, Associated Regional and University Pathologists; apoE, apolipoprotein E; T_m, melting temperature.

knowledge of mutation frequency in some regions, creating a suitable panel for ethnically diverse populations is challenging. Three years after their initial recommendation, the ACMG revised their recommendation to include only 23 variants *(4)*.

Complete analysis of *CFTR* may be used in affected patients when 2 disease alleles are not identified by genotyping assays. Complete gene analysis is seldom recommended as a screening assay because novel variants may be difficult to interpret and can complicate genetic counseling. Furthermore, sequencing remains expensive. Alternatively, scanning techniques have been used to identify *CFTR* variants, including denaturing gradient gel electrophoresis *(5, 6)*, single-strand conformation polymorphism analysis *(7, 8)*, denaturing HPLC *(9, 10)*, temperature gradient gel electrophoresis *(11)*, and temperature gradient capillary electrophoresis *(12)*. Despite their high degree of accuracy and relatively low cost, the labor-intensive nature of these techniques restricts their use to research and selected reference laboratories.

Recently, high-resolution melting analysis was introduced as a simple, closed-tube, gene scanning technique *(13)*. Sensitivity and specificity appear better than those of denaturing HPLC *(14)* and approach 100% for PCR products <400 bp *(15)*. All heterozygotes and most homozygotes can be detected without mixing *(16, 17)*, although p.F508del is not distinguished from wild-type *(14)*.

On the basis of the finding that common benign variants can be identified from normal samples *(18)*, we used high-resolution melting to decrease the sequencing burden by using melting patterns to identify and eliminate common variants. We also explored the possibility that most disease-causing variants have unique melting profiles, suggesting that direct genotyping by amplicon melting may be possible. We also aimed to develop specific genotyping assays that can be performed under the same conditions as amplicon scanning for cases in which amplicon melting yielded ambiguous results.

Materials and Methods

DNA SAMPLES

A human random control DNA panel (HRC-1) of 96 white blood donors from the UK was obtained from the European Collection of Cell Cultures. In addition, extracted DNA from 96 human blood samples submitted to Associated Regional and University Pathologists (ARUP) for apolipoprotein E (apoE) genotyping was kindly deidentified according to a global ARUP protocol (institutional review board no. 7275). Samples used in the blinded portions of this study (n = 30) were selected from the Coriell Institute for Medical Research and from a prior study of cystic fibrosis genotyping *(19)*.

PRIMERS

Primers were designed by use of LightScanner® primer design software (Idaho Technology) and synthesized by the University of Utah core synthesis facility. All 27 exons of *CFTR* and adjacent intron/exon junctions were amplified in 36 reactions, producing products of 146–322 bp. An additional 206-bp region of intron 19 was amplified to scan for the 3849 + 10kbC>T variant recommended for testing by the ACMG. As much as possible, benign variants within introns were excluded (e.g., the TTGA repeat in intron 6a), whereas most reported disease-causing splice variants were included. The forward primer for exon 9 was designed within the exon boundary to avoid the poly(GT) and poly(T) tracts in intron 8 that are often heterozygous. To maximize sensitivity, exons 4, 7, 13, 15, 17b, 19, and 24 were each split into multiple amplicons. Sequences of the PCR primers and amplicon lengths are listed in Table 1 in the Data Supplement that accompanies the online version of this article at http://www.clinchem.org/content/vol53/issue11.

PCR

PCR was performed in 96-well microtiter plates in 10-μL volumes. Reactions included 25 ng of genomic DNA in 50 mmol/L Tris (pH 8.3) with 2 mmol/L $MgCl_2$, 0.2 mmol/L each deoxynucleoside triphosphate, 500 mg/L BSA, 1× LCGreen® PLUS (Idaho Technology), 0.4 U KlenTaq1™ (AB Peptides), 88 ng of TaqStart™ antibody (Clontech), and 0.5 μmol/L of each primer. To ease assay assembly, the variable reagent was dried in the plate wells and stored. The common PCR reagents were then added at a later time by addition of a master mix. In the studies presented here, template DNA was dried in the plates. However, when only a few samples are studied, it is more convenient to dry the primer sets in different wells.

Reactions were overlaid with 10 μL of mineral oil (Sigma), the plates were centrifuged (1500*g* for 3–5 min), and PCR was performed in a PTC-200 thermal cycler (Bio-Rad) with an initial denaturation at 95 °C for 5 min, followed by 36 cycles of 95 °C for 30 s, 62 °C for 10 s, and 72 °C for 30 s. To promote heteroduplex formation, samples were subsequently denatured by heating to 95 °C for 30 s and cooled to 15 °C.

MELTING ANALYSIS

After PCR, the plates were centrifuged (1500*g* for 3–5 min) and imaged in a 96-well LightScanner (Idaho Technology). The plates were heated at 0.1 °C/s, and fluorescence was collected from 60 to 95 °C. Melting curves were analyzed by methods detailed elsewhere *(18, 20, 21)*, either on custom software or with commercial LightScanner software. Briefly, after exponential background subtraction *(22)*, melting curves were normalized between 0% and 100%. Minor temperature differences between samples were corrected by superimposing curves in regions of low fluorescence (2%–5% normalized fluorescence). Normalized and temperature-overlaid curves were viewed on difference plots to magnify variations in melting curve shape. Difference plots were generated by subtracting each curve from the mean wild-type curve, defined as the most common genotype. Clustering of melting curves for

genotype identification was performed manually, aided by unbiased, hierarchal clustering using mean absolute difference metrics *(18)* or commercial LightScanner software on the high sensitivity setting. Predicted melting temperature (T_m) profiles used a Poland-Scheraga model for base-pairing probability profiles *(23)*.

SEQUENCING

The genotype of all variant clusters was determined by standard bidirectional fluorescent sequencing (University of Utah Core Laboratory). Genotype homogeneity within clusters was confirmed by sequencing any samples on the edge of apparent clusters.

PRELIMINARY OPTIMIZATION

The 96 apoE DNA samples were used for initial assay optimization and final primer selection. Two previously unreported variants (c.605G>C in exon 4 and c.3891G>A in exon 20) were identified during this initial optimization (Table 1; data not shown).

Table 1. Variants identified in random panels.[a]

Exon	cDNA (c.)	Protein (p.)	Allele fraction (%)
1	125G>C		3.8
3	356G>A	R75Q	3.5
4	605G>C	S158T	<0.4[b,c]
6b	1001 + 11C>T		13.1
10	1540A>G	M470V	30.0[d]
	1716G>A		1.5
12	1859G>C	G576A	1.5
13	2134C>T	R668C	1.5
14a	2694T>G		26.2
14b	2752 − 6T>C		0.4
15	3032T>C	L967S	0.8
17b	3417A>T	T109S	1.5
19	3601 − 17T>C		0.4
20	3891G>A		<0.4[b,c]
	4002A>G		1.5
21	4029A>G		0.4
23	4294C>G	L1388V	0.4[b]
	4316G>A	C1395Y	0.4[b]
	4374 + 13A>G		0.4
24	4404C>T		0.8
	4521G>A		20.8

[a] All variants were identified by scanning random panels and confirmed by sequencing. Unless specified otherwise, each allele was identified in the HRC-1 panel and the allele fraction was calculated from both the HRC-1 and the blinded 30 sample analysis (252 chromosomes). Two F508del heterozygotes were also found in the HRC-1 panel but are not tabulated here. Translation starts at c.133 of the *CFTR* cDNA sequence in GenBank NM_000492.

[b] Previously unreported variant.

[c] Identified in a random panel screen of 96 deidentified DNA samples used for assay optimization that were submitted to ARUP for apoE genotyping. These variants were not present in the normal HRC-1 or blinded 30 samples otherwise reported here.

[d] The allele fraction was calculated from the 30 sample blinded panel using an unlabeled probe assay *(24)*.

GENOTYPING ASSAYS

Specific genotyping assays were developed for the heterozygotes in exons 10, 11, and 20 that could not be differentiated, for homozygous p.508del and for the 5T allele of the poly(T) tract in intron 8. These assays were designed as either unlabeled probe *(24)* or small amplicon *(16)* melting assays, using the same PCR conditions, saturating DNA dye, and melting equipment as the scanning assays.

Results

CFTR was scanned by high-resolution melting after PCR amplification of 37 exon/intron fragments in each of 126 human DNA samples. An initial panel of 96 random white UK blood donors was used to correlate common variants with melting patterns. Subsequently, a blinded 30-sample panel enriched for disease-causing variants was studied to assess sensitivity. Amplification in 96-well plates in the presence of a saturating DNA dye was successful 99.8% of the time. The 9 wells with poor amplification were identified by fluorescent imaging of the plate before melting acquisition. The reactions that did not amplify well occurred randomly, and all were successfully amplified on a 2nd attempt. Complete data sets of normalized melting curves, difference plots, and plate maps of the 96 random and 30 blinded samples are provided in Figs. 1 and 2, respectively, in the online Data Supplement.

Typical normalized melting plots and plate maps from the random panel are shown in Fig. 1. All samples in the most common genotype cluster together after normalization and curve overlay. Heterozygous samples have a different shape from that of the common homozygous cluster, with low-temperature deviations resulting from heteroduplexes. When the samples are ordered according to plate position, similar patterns on 8 × 12 plate maps indicate allele associations, such as the haplotype association observed in Fig. 1.

Twenty-two variant alleles were identified in the random panel (Table 1). The disease-causing p.F508del was detected in 2 samples. No variants were observed in 12 exons and the intron 19 amplicon, and 1 variant was detected in 12 exons, 2 variants in exons 10 and 24, and 3 variants in exon 23. Four variants had an allele fraction >10% (c.1001 + 11C>T, c.1540A>G, c.2789 + 5G>A, and c.4521G>A), and 2 others, >3% (c.125G>C and c.356G>A). Four variants (p.S158T, c.3891G>A, p.L1388V, and p.C1395Y) have not been reported previously, and each was detected in only a single sample.

Melting analysis for a typical exon in the blinded study is shown in Fig. 2. Thirty normalized melting curves are shown in Fig. 2A, revealing 2 unique variants. Difference plots provide magnification for easier visualization and discrimination (Fig. 2B). The 2 variants displace different portions of the melting curve because they occur in different regions of thermal stability. This regional thermal stability can be predicted and plotted against position

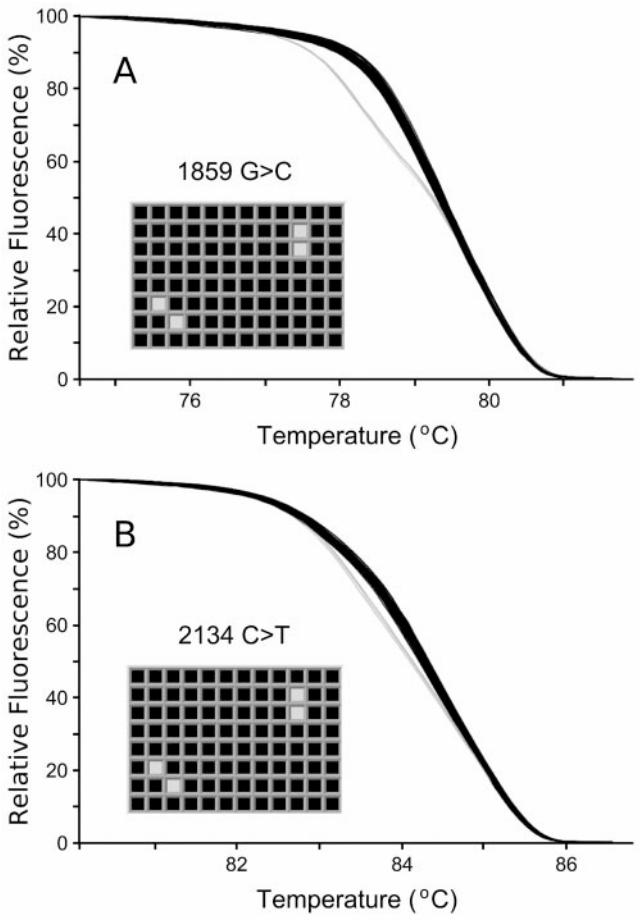

Fig. 1. Normalized melting curves and plate maps from 2 *CFTR* exons after temperature overlay.

Samples from 96 random blood donors were PCR amplified and analyzed by high-resolution melting. The exon 12 amplicon shown in (*A*) was 169 bp, and the exon 13 fragment shown in (*B*) was 322 bp. Aberrant melting profiles reveal the presence of 2 heterozygous variants, c.1859G>C in exon 12 and 2134C>T in exon 13, that are present in the same 4 samples. The identical plate position of the variants indicates that in this population they are inherited as a haplotype.

as displayed in the T_m profile of Fig. 2C *(23)*. p.G85E is in a region of lower stability and the change in melting curve shape is most distinctive at lower temperatures. In contrast, the p.R75X variant occupies a region of greater thermal stability and exhibits a shape change at higher temperatures.

The disease-associated variants tested in the blinded study are shown in Table 2. All 23 variants recommended for genotyping by the ACMG are included, as well as 8 additional variants associated with disease. The complete genotype of all 30 samples is given in Table 2 in the online Data Supplement.

Scanning identified all 40 amplicons with heterozygous disease-causing variants (100% sensitivity for disease-causing variants in the heterozygous state). Of these 40 amplicons, 29 contained unique variants. In addition, scanning identified another 47 amplicons as heterozygous. When the melting profiles of the 6 most common heterozygotes from the random panel were considered,

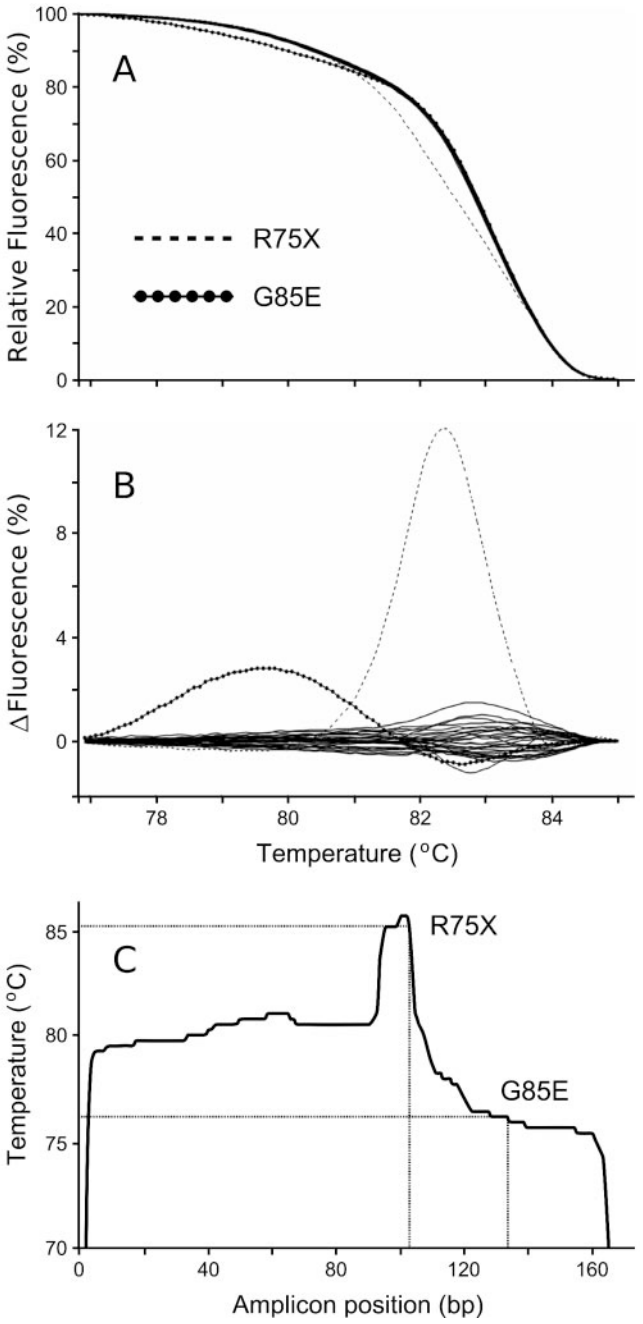

Fig. 2. Unique melting profiles of disease-causing variants found in exon 3 of *CFTR*.

In (*A*), 30 normalized and overlaid fluorescence *curves* reveal the presence of 2 heterozygous variants that uniquely deviate from the wild-type cluster. In (*B*), to make the deviations more apparent the same data are plotted as the difference of each curve from the mean homozygous wild-type. In (*C*), a T_m profile *(23)* of the amplicon reveals that the variants occur in different regions of thermal stability. G85E is in a low-temperature domain compared with R75X, resulting in deviation of the melting curves at different temperatures. The PCR product was 169 bp in length.

45 false positives were avoided. The 2 remaining false positives, c.4002A>G in exon 20 and c.4404C>T in exon 24, were less common benign variants. A previously unreported probable splicing variant, c.3500-2A>T, was

Table 2. Disease-associated variants detected in 30 blinded samples.[a]

Exon	cDNA (c.)	Protein (p.)
2	223C>T	R31C
3	355C>T	R75X
	386G>A	**G85E**
4	**482G>A**	**R117H**
	575T>C	I148T
	621 + 1G>T[b]	
5	**711 + 1G>T**	
7	1078delT	
	1132C>T	**R334W**
	1150delA	
	1172G>C	**R347P**
8	1341 + 18A>C[c]	
9	**1496C>A**	**A455E**
10	**1651–1653del**	**I507del**
	1653–1655del	**F508del**[d]
11	**1717 − 1G>A**	
	1756G>T	**G542X**[e]
	1784G>A	**G551D**[b]
	1789C>T	**R553X**[f]
	1811G>C	**R560T**
12	**1898 + 1G>A**	
13	**2184delA**	
14b	**2789 + 5G>A**[e]	
16	**3120 + 1G>A**	
18	3500 − 2A>T[g]	
19	**3616C>T**	**R1162X**
	3659delC	
Intron 19	**3849 + 10kbC>T**[e]	
20	**3978G>A**	**W1282X**
21	**4041C>G**	**N1303K**
22	4178G>A	G1349D[c]

[a] Disease-causing variants recommended for genotyping by the ACMG *(4)* are in bold. All variants were detected only once as heterozygotes unless specified. The complete genotypes of the 30 samples tested are given in Supplemental Data Table 2.

[b] Three samples were heterozygous.

[c] c.1341 + 18A>C was associated with the variant p.G1349D in 1 sample.

[d] In addition to 9 p.F508del heterozygous samples that were detected, 1 p.F508del homozygote was not detected as expected from a prior study *(14)*.

[e] Homozygous sample.

[f] Two samples were heterozygous.

[g] Novel (presumed disease-causing) variant.

identified as the 2nd allele of a Coriell sample (NA12960) from a patient with disease.

In addition to heterozygotes, some homozygous variants are detected by high-resolution melting analysis (Fig. 3). The homozygous c.4521G>A genotype separates from the wild-type, although the magnitude of the deviation is not as great as for the heterozygote (Fig. 3A). Similarly, the homozygotes of 2 other common variants, c.1001 + 11C>T and c.2694T>G, were easily distinguished (see Figs. 1 and 2 in the online Data Supplement). Furthermore, 3 homozygous disease-causing variants were identified in the blinded study: p.G542X, c.2789 + 5G>A, and c.3849 + 10kbC>T.

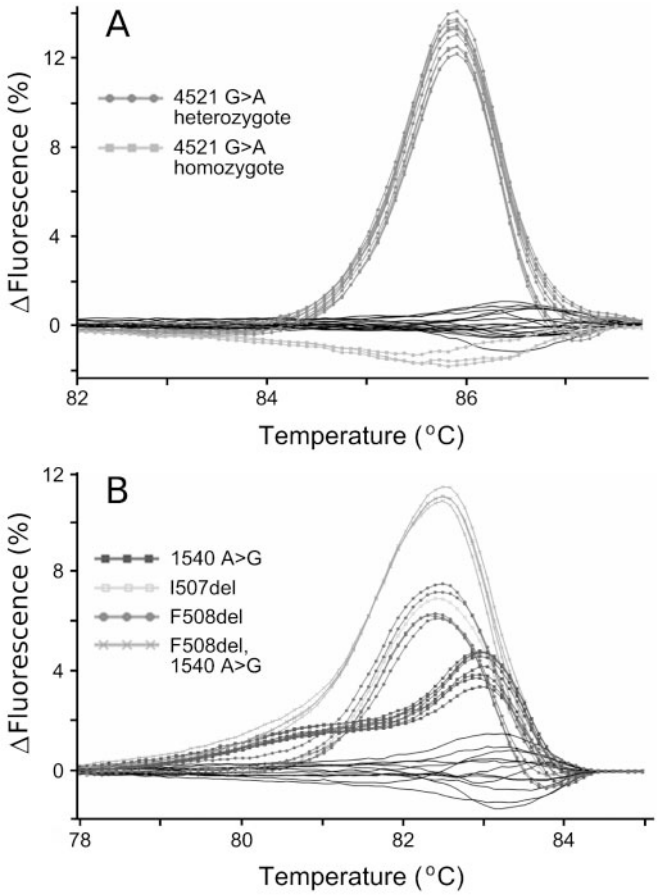

Fig. 3. Some, but not all, homozygous sequence variants can be distinguished from wild-type.

Melting curve difference *plots* (after normalization and overlay) of 30 blinded samples enriched for disease-causing variants are shown. In (*A*), both heterozygous and homozygous genotypes of c.4521G>A can be distinguished within a 151-bp product. In (*B*), 4 melting curve clusters of a 277-bp product including exon 10 are apparent. The wild-type cluster includes 3 c.1540A>G and 1 p.F508del homozygotes, in addition to several wild-type samples. The c.1540A>G heterozygotes are clearly separated from the p.F508del heterozygotes and the c.1540A>G/p.F508del double heterozygotes. However, the p.F508del and p.I507del heterozygotes are in the same cluster.

Not all homozygous variants are distinguishable from each other, however. The 2 exceptions both occurred in exon 10 (Fig. 3B). Homozygous variants of either the benign c.1540A>G or the disease-causing p.F508del clustered with normal samples. Homozygous p.F508del can be genotyped by mixing with a known genotype *(17)* either before or after PCR (data not shown) or by unlabeled probe analysis (see Fig. 3 in the online Data Supplement). In total, 6 of 8 homozygous genotypes were detected for a homozygous variant detection sensitivity of 75%.

Most heterozygous variants were distinguishable from each other by the unique shape of their melting profiles. A difference plot of the variants found in exon 11 is shown in Fig. 4. Six different alleles and 7 unique genotypes are present. Each genotype traces a different path, with the exception of p.G551D and p.R553X. Considering all *CFTR*

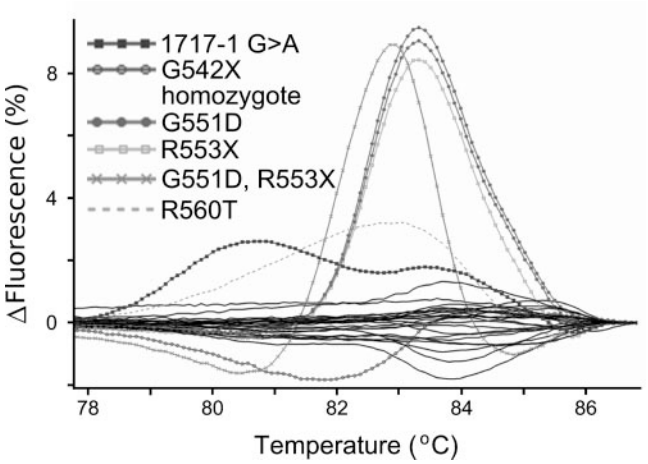

Fig. 4. Exon 11 difference plots (after normalization and overlay) of 30 blinded samples enriched for disease-causing variants.

Six genotypes other than wild-type are present. With the exception of p.G551D and p.R553X, the melting profile of each genotype is distinct, including the G542X homozygote. The PCR product was 175 bp in length.

amplicons, 37 of 40 pairwise comparisons between different heterozygotes could be distinguished. The exceptions included 3-bp deletions, p.I507del/p.F508del, and 2 single-base variant pairs (p.G551D/p.R553X and p.W1282X/c.4002A>G). Specific genotyping assays that distinguish these variants are detailed in Figs. 3–5 in the online Data Supplement. Fig. 3 in the online Data Supplement demonstrates an unlabeled probe assay to differentiate heterozygous p.I507del from heterozygous p.F508del, as well as homozygous p.F508del from wild-type. Fig. 4 in the online Data Supplement details an unlabeled probe assay to differentiate p.G551D from p.R553X. Fig. 5 in the online Data Supplement describes a small amplicon assay to distinguish the disease-causing variant p.W1282X from the benign variant c.4002A>G.

Because the primers for exon 9 avoided the poly(GT) and poly(T) tracts in intron 8, a separate unlabeled probe assay was developed to detect the clinically relevant 5T allele. With a probe complementary to the 5T allele, 7T and 9T alleles form internal bulge loops that result in duplexes with lower melting transitions than the 5T allele (see Fig. 6 in the online Data Supplement).

Discussion

High-resolution DNA melting is a new method for sequence-variant scanning that has been recently reviewed *(25, 26)*. The sensitivity and specificity for this method, although dependent on the instrument and the dye used *(27–29)*, appear superior to other scanning methods *(14)*. The technique is attractive because it is simple, nondestructive, and amendable to high-throughput on 96- or 384-well plates. Because there is no need for additions or processing after PCR, the samples never leave the microtiter plate and there is no contamination risk. Real-time PCR is not necessary.

High-resolution melting was used to scan *CFTR*, including intron/exon junctions and a segment of intron 19 to include all ACMG mutations. Thirty-seven amplicons were used with PCR product lengths between 146 and 322 bps. This length restriction was based on a prior study that reported 100% sensitivity and specificity for heterozygous single-base substitutions in amplicons <400 bp *(15)*. In our blinded study, scanning detected all 40 disease-associated heterozygotes for a sensitivity of 100%. However, 47 benign heterozygotes were also detected. In total, 8.7% of the amplicons were heterozygous. If all heterozygous amplicons are sequenced, more benign variants than disease-causing variants are analyzed, even in a population highly enriched for disease-causing variants.

Common benign variants interfere with heteroduplex scanning methods because all variants are detected, whether or not they cause disease. This situation increases the sequencing workload and decreases the utility of scanning. A recent report suggests that analysis of a healthy population can identify common variants by their characteristic melting patterns *(18)*. Therefore, we identified common *CFTR* variants by scanning a random human DNA panel of 96 samples. Twenty-one apparent benign variants were identified, but only 6 had an allele frequency >0.02. The identity and frequency of variants were similar to those reported previously *(30)*, although 4 novel variants were identified. Using the melting patterns of the 6 most common heterozygotes, we eliminated 45 of 47 benign variants from consideration. Therefore, in our 30 blinded samples, only 2 of 1110 amplicons contained rare benign variants that were not matched to common variants observed in the random population.

The melting profiles obtained by high-resolution melting are often unique to specific variants *(13, 31)*. How a heterozygote alters the melting-curve shape depends on the nature of the heterozygote (i.e., the specific base mismatch), as well as the thermal stability around the variant. For example, Fig. 2 demonstrates the effect of surrounding thermal stability. Although the variants are the same mismatch type *(16)* and are only 31 bases apart, they are surrounded by regions that differ in thermal stability. As a result, the 2 variants perturb the melting curve at different temperatures and are readily distinguishable. Heterozygotes resulting from deletions and single-base substitutions of different types *(16)* produce heteroduplexes of varying stability that also uniquely affect the melting curve. In 1 prior study with small amplicons, all 21 random pairs of heterozygotes studied were distinguishable *(31)*.

Not all heterozygous variants produce unique melting curves by amplicon scanning, however. For example, identical nearest neighbor changes may occur at different locations in the same amplicon, such as identical base changes at multiple cysteine residues in the RET protooncogene *(32)*. In this study, 37 of 40 pairs of heterozygotes were distinguishable (93%) when they were in the same amplicon. The exceptions included a pair of 3 base dele-

tions very close to each other (p.I507del and p.F508del), and 2 pairs of single-nucleotide substitutions. The substitutions were 5 bp (p.G551D and p.R553X) and 24 bp (p.W1282X and c.4002A>G) apart, and the variants within each pair were of the same type *(16)*. These exceptions can be genotyped with simple unlabeled probe and/or small amplicon melting assays run under the same conditions as the amplicon-scanning assays (see Figs. 3–5 in the online Data Supplement). Furthermore, an ancillary unlabeled probe assay to detect the 5T allele of the poly(T) tract in intron 8 was developed (see Fig. 6 in the online Data Supplement).

Most scanning technologies do not identify homozygous variants. High-resolution melting is in an exception in that many homozygotes are detected. In this study, 6 of 8 homozygous variants were clearly separated from wild-type, although the melting curve displacement was small compared with heterozygous variants. The detection of homozygous variants by this method implies that the melting curve shape is altered, not just its position along the temperature axis. One of the homozygous variants not detected was the common *CFTR* benign variant, c.1540A>G. Not detecting this common homozygote simplifies the melting pattern of benign variants and makes it easier to identify disease-causing variants (Fig. 3). The other homozygote not detected by amplicon scanning is the most common disease-causing variant, p.F508del *(14)*. Many techniques to genotype the p.F508del locus are available [e.g., *(19*, *33)*], and it seems prudent to genotype at least this locus before attempting full gene analysis. Quantitative heteroduplex analysis *(17)* and unlabeled probes (see Fig. 3 in the online Data Supplement) are attractive options for genotyping because they can use the same PCR and melting protocols used for amplicon scanning. Another option is simultaneous scanning and genotyping with unlabeled probes in the same reaction *(34)*.

There are several practical limitations to scanning by amplicon melting. For highest accuracy, controls must be on the same plate, because between-run variation is greater than within-run variation. Furthermore, because heterozygote scanning is a comparative method, accuracy increases with the number of samples analyzed in a single run. These concerns may be addressed by use of a 384-well plate format to analyze several samples at once, along with at least the 6 most common variants to decrease the sequencing load.

Additional design limitations arise from avoiding the poly(GT) and poly(T) tracts within intron 8 to eliminate heteroduplexes from these repeats. As a result, rare disease-causing variants near the intron 8/exon 9 junction will not be identified. Furthermore, rare splice variants outside our primers or deep within exons will be missed, although we specifically designed an assay to detect the 3849 + 10kbC>T variant. Finally, deletions of one or more exons, estimated to occur at a frequency of 1%–3% in disease-causing chromosomes *(35)*, will not be detected and could make the scanning of hemizygous variants within the deleted area more difficult.

Despite these limitations, high-resolution melting is a simple and rapid method for comprehensive analysis of *CFTR*, offering speed, low cost, and a high degree of accuracy compared with other scanning techniques. Labor requirements can be decreased by using plates with the oligonucleotides already dried in the wells. The cost of scanning 1 sample as described here is approximately $12 in PCR reagents and disposables, including the saturating DNA dye that accounts for approximately one-sixth of the total cost. One major cost of any scanning method is reflexive sequencing. Decreasing false-positive results by identifying common variants and genotyping disease-causing variants by their melting signatures are 2 options that decrease sequencing requirements. The risk of error when 2 different heterozygotes are in the same amplicon (e.g., misclassifying a rare variant as a common variant or the inability to distinguish 2 disease-causing variants) appears to be approximately 7%. In our blinded study of 30 samples, no misclassification errors were made. If greater accuracy is required, ancillary small amplicon *(16*, *36)* and unlabeled probe *(24)* genotyping or simultaneous scanning and genotyping with unlabeled probes *(34)* are options that can be performed on the same platform, either sequentially or in parallel. After DNA purification, PCR amplification and high-resolution melting requires only approximately 2 h on 96- or 384-well plates.

Grant/funding support: This work was supported by National Institutes of Health Grants GM072419 and GM073396 and a Center of Excellence Grant from the State of Utah.
Financial disclosures: Aspects of high-resolution melting analysis are licensed from the University of Utah to Idaho Technology. C.T.W. holds equity interest in Idaho Technology.
Acknowledgments: We thank ARUP for providing deidentified clinical samples.

References

1. Riordan JR, Rommens JM, Kerem B, Alon N, Rozmahel R, Grzelczak Z, et al. Identification of the cystic fibrosis gene: cloning and characterization of complementary DNA. Science 1989;245:1066–73.
2. Bobadilla JL, Macek M Jr, Fine JP, Farrell PM. Cystic fibrosis: a worldwide analysis of CFTR mutations: correlation with incidence data and application to screening. Hum Mutat 2002;19:575–606.
3. Grody WW, Cutting GR, Klinger KW, Richards CS, Watson MS, Desnick RJ. Laboratory standards and guidelines for population-based cystic fibrosis carrier screening. Genet Med 2001;3:149–54.
4. Watson MS, Cutting GR, Desnick RJ, Driscoll DA, Klinger K, Mennuti M, et al. Cystic fibrosis population carrier screening: 2004 revision of American College of Medical Genetics mutation panel. Genet Med 2004;6:387–91.

5. Fanen P, Ghanem N, Vidaud M, Besmond C, Martin J, Costes B, et al. Molecular characterization of cystic fibrosis: 16 novel mutations identified by analysis of the whole cystic fibrosis conductance transmembrane regulator (CFTR) coding regions and splice site junctions. Genomics 1992;13:770–6.
6. Wu Y, Hofstra RM, Scheffer H, Uitterlinden AG, Mullaart E, Buys CH, et al. Comprehensive and accurate mutation scanning of the CFTR gene by two-dimensional DNA electrophoresis. Hum Mutat 1996;8:160–7.
7. Claustres M, Laussel M, Desgeorges M, Giansily M, Culard JF, Razakatsara G, et al. Analysis of the 27 exons and flanking regions of the cystic fibrosis gene: 40 different mutations account for 91.2% of the mutant alleles in southern France. Hum Mol Genet 1993;2:1209–13.
8. Dork T, Mekus F, Schmidt K, Bosshammer J, Fislage R, Heuer T, et al. Detection of more than 50 different CFTR mutations in a large group of German cystic fibrosis patients. Hum Genet 1994; 94:533–42.
9. Le Marechal C, Audrezet MP, Quere I, Raguenes O, Langonne S, Ferec C. Complete and rapid scanning of the cystic fibrosis transmembrane conductance regulator (CFTR) gene by denaturing high-performance liquid chromatography (D-HPLC): major implications for genetic counselling. Hum Genet 2001;108:290–8.
10. Ravnik-Glavac M, Atkinson A, Glavac D, Dean M. DHPLC screening of cystic fibrosis gene mutations. Hum Mutat 2002;19:374–83.
11. Wong LJ, Alper OM. Detection of CFTR mutations using temporal temperature gradient gel electrophoresis. Electrophoresis 2004; 25:2593–601.
12. Chou LS, Gedge F, Lyon E. Complete gene scanning by temperature gradient capillary electrophoresis using the cystic fibrosis transmembrane conductance regulator gene as a model. J Mol Diagn 2005;7:111–20.
13. Wittwer CT, Reed GH, Gundry CN, Vandersteen JG, Pryor RJ. High-resolution genotyping by amplicon melting analysis using LCGreen. Clin Chem 2003;49:853–60.
14. Chou LS, Lyon E, Wittwer CT. A comparison of high-resolution melting analysis with denaturing high-performance liquid chromatography for mutation scanning: cystic fibrosis transmembrane conductance regulator gene as a model. Am J Clin Pathol 2005; 124:330–8.
15. Reed GH, Wittwer CT. Sensitivity and specificity of single-nucleotide polymorphism scanning by high-resolution melting analysis. Clin Chem 2004;50:1748–54.
16. Liew M, Pryor R, Palais R, Meadows C, Erali M, Lyon E, et al. Genotyping of single-nucleotide polymorphisms by high-resolution melting of small amplicons. Clin Chem 2004;50:1156–64.
17. Palais RA, Liew MA, Wittwer CT. Quantitative heteroduplex analysis for single nucleotide polymorphism genotyping. Anal Biochem 2005;346:167–75.
18. Vandersteen JG, Bayrak-Toydemir P, Palais RA, Wittwer CT. Identifying common genetic variants by high-resolution melting. Clin Chem 2007;53:1191–8.
19. Wittwer CT, Marshall BC, Reed GH, Cherry JL. Rapid cycle allele-specific amplification: studies with the cystic fibrosis delta F508 locus. Clin Chem 1993;39:804–9.
20. Montgomery J, Wittwer CT, Palais R, Zhou L. Simultaneous mutation scanning and genotyping by high-resolution DNA melting analysis. Nat Protoc 2007;2:59–66.
21. Gundry CN, Vandersteen JG, Reed GH, Pryor RJ, Chen J, Wittwer CT. Amplicon melting analysis with labeled primers: a closed-tube method for differentiating homozygotes and heterozygotes. Clin Chem 2003;49:396–406.
22. Erali M, Palais B, Wittwer C. SNP genotyping by unlabeled probe melting analysis. In: Seitz O, Marx A, eds. Molecular Beacons: Signaling Nucleic Acid Probes, Methods and Protocols, Methods in Molecular Biology, Vol. 429. Totowa, NJ: Humana Press, 2007;199–206.
23. Tostesen E, Liu F, Jenssen TK, Hovig E. Speed-up of DNA melting algorithm with complete nearest neighbor properties. Biopolymers 2003;70:364–76.
24. Zhou L, Myers AN, Vandersteen JG, Wang L, Wittwer CT. Closed-tube genotyping with unlabeled oligonucleotide probes and a saturating DNA dye. Clin Chem 2004;50:1328–35.
25. Dujols VE, Kusukawa N, McKinney JT, Dobrowolski SF, Wittwer CT. High-resolution melting analysis for scanning and genotyping. In: Dorak MT, ed. Real-Time PCR. New York: Garland Science 2006; 157–71.
26. Reed GH, Kent JO, Wittwer CT. High-resolution DNA melting analysis for simple, efficient molecular diagnostics. Pharmacogenomics 2007;8:597–608.
27. Herrmann MG, Durtschi JD, Bromley LK, Wittwer CT, Voelkerding KV. Amplicon DNA melting analysis for mutation scanning and genotyping: cross-platform comparison of instruments and dyes. Clin Chem 2006;52:494–503.
28. Herrmann MG, Durtschi JD, Bromley LK, Wittwer CT, Voelkerding KV. Instrument comparison for heterozygote scanning of single and double heterozygotes: a correction and extension of Herrmann et al., Clin Chem 2006;52:494–503. Clin Chem 2007;53: 150–2.
29. Herrmann MG, Durtschi JD, Wittwer CT, Voelkerding KV. Expanded instrument comparison of amplicon DNA melting analysis for mutation scanning and genotyping. Clin Chem 2007;53:1544–8.
30. Modiano G, Bombieri C, Ciminelli BM, Belpinati F, Giorgi S, Georges M, et al. A large-scale study of the random variability of a coding sequence: a study on the CFTR gene. Eur J Hum Genet 2005;13:184–92.
31. Graham R, Liew M, Meadows C, Lyon E, Wittwer CT. Distinguishing different DNA heterozygotes by high-resolution melting. Clin Chem 2005;51:1295–8.
32. Margraf RL, Mao R, Highsmith WE, Holtegaard LM, Wittwer CT. RET proto-oncogene genotyping using unlabeled probes, the masking technique, and amplicon high-resolution melting analysis. J Mol Diagn 2007;9:184–96.
33. Gundry CN, Bernard PS, Herrmann MG, Reed GH, Wittwer CT. Rapid F508del and F508C assay using fluorescent hybridization probes. Genet Test 1999;3:365–70.
34. Zhou L, Wang L, Palais R, Pryor R, Wittwer CT. High-resolution DNA melting analysis for simultaneous mutation scanning and genotyping in solution. Clin Chem 2005;51:1770–7.
35. Schneider M, Joncourt F, Sanz J, von Kanel T, Gallati S. Detection of exon deletions within an entire gene (CFTR) by relative quantification on the LightCycler. Clin Chem 2006;52:2005–12.
36. Dobrowolski SF, Ellingson C, Coyne T, Grey J, Martin R, Naylor EW, et al. Mutations in the phenylalanine hydroxylase gene identified in 95 patients with phenylketonuria using novel systems of mutation scanning and specific genotyping based upon thermal melt profiles. Mol Genet Metab 2007;91:218–27.